RESEARCH ARTICLE

JCN RESEARCH IN SYSTEMS NEUROSCIENCE
THE JOURNAL OF COMPARATIVE NEUROLOGY

WILEY

# Expression and localization of neuronal nitric oxide synthase in the brain and sensory tissues of the African cichlid fish *Astatotilapia burtoni*

Robert B. Mobley [ID] | Emily J. Ray [ID] | Karen P. Maruska [ID]

Department of Biological Sciences, Louisiana State University, Baton Rouge, Louisiana, USA

**Correspondence**
Robert B. Mobley, Department of Biological Sciences, Louisiana State University, 202 Life Sciences Bldg., Baton Rouge, LA 70803, USA.
Email: rmobley@lsu.edu

## Abstract

Nitric oxide (NO) produced by the enzyme neuronal nitric oxide synthase serves as an important neurotransmitter in the central nervous system that is involved in reproductive regulation, learning, sensory processing, and other forms of neural plasticity. Here, we map the distribution of *nnos*-expressing cells in the brain and retina of the cichlid fish *Astatotilapia burtoni* using in situ hybridization. In the brain, *nnos*-expressing cells are found from the olfactory bulbs to the hindbrain, including within specific nuclei involved in decision-making, sensory processing, neuroendocrine regulation, and the expression of social behaviors. In the retina, *nnos*-expressing cells are found in the inner nuclear layer, presumably in amacrine cells. We also used quantitative PCR to test for differences in *nnos* expression within the eye and olfactory bulbs of males and females of different reproductive states and social statuses. In the eye, males express more *nnos* than females, and socially dominant males express more *nnos* than subordinate males, but expression did not differ among female reproductive states. In the olfactory bulbs, dominant males had greater *nnos* expression than subordinate males. These results suggest a status-specific function for NO signaling in the visual and olfactory systems that may be important for sensory perception related to mating or territorial interactions to maintain the social hierarchy. The widespread distribution of *nnos*-expressing cells throughout the cichlid brain is similar to that in other teleosts, with some conserved localization patterns across vertebrates, suggesting diverse functions for this important neurotransmitter system.

**KEYWORDS**
in situ hybridization, olfactory, reproduction, retina, teleost

**Abreviations:** 4v, fourth ventricle; ac, anterior commissure; aGn, anterior glomerular nucleus; An, anterior thalamic nucleus; AON, anterior octaval nucleus; AP, accessory pretectal nucleus; ATn, anterior tuberal nucleus; CCeG, granular layer of corpus cerebelli; CCeM, molecular layer of corpus cerebelli; CCeP, purkinje layer of corpus cerebelli; CG, central gray; CM, corpus mammillare; DON, descending octaval nucleus; DWZ, deep white zone of tectum; EG, eminentia granularis; FL, Facial lobe; GCL, ganglion cell layer of the retina; Gn, glomerular nucleus; hc, horizontal commissure; ICL, internal cell layer of olfactory bulb; INL, inner nuclear layer of the retina; IPL, inner plexiform layer of the retina; LFB, lateral forebrain bundle; MFN, medial funicular nucleus; mlf, medial longitudinal fasciculus; MON, medial octavolateralis nucleus; NCC, commissural nucleus of Cajal; nHd, dorsal habenular nucleus; nHv, ventral habenular nucleus; NLT, lateral tuberal nucleus; NLTd, lateral tuberal nucleus, dorsal part; NLTi, lateral tuberal nucleus, intermediate part; NLTl, lateral tuberal nucleus, lateral part; NLTm, lateral tuberal nucleus, medial part; NLTv, lateral tuberal nucleus, ventral part; NLVc, ventral part of nucleus of the lateral valvulae; nMLF, nucleus of medial longitudinal fasciculus; nMMp, magnocellular preoptic nucleus, magnocellular division; nPMp, magnocellular preoptic nucleus, parvocellular division; nPPa, parvocellular preoptic nucleus, anterior part; nPPp, parvocellular preoptic nucleus, posterior part; NPT, posterior tuberal nucleus; NRL, nucleus of the lateral recess; NRP, nucleus of the posterior recess; NT, nucleus taenia; OB, olfactory bulb; oc, optic chiasm; ON, optic nerve; ONL, outer nuclear layer of the retina; OPL, outer plexiform layer of the retina; pc, posterior commissure; PGa, anterior preglomerular nucleus; PGc, commissural preglomerular nucleus; PGl, lateral preglomerular nucleus; PGm, medial preglomerular nucleus; PGZ, periventricular gray zone of tectum; PL, photoreceptor layer of the retina; POA, preoptic area; PS, pineal stalk; PSP, parvocellular superficial pretectal nucleus; SGn, secondary gustatory nucleus; sgt, secondary gustatory tract; smn, spinal motor neurons; SR, superior raphe nucleus; SWGZ, superficial gray and white zone of tectum; T, tectum; TL, torus longitudinalis; TS, torus semicircularis; VL, vagal lobe; VMn, ventromedial thalamic nucleus; VOT, ventral optic tract.

# 1 | INTRODUCTION

The central nervous system (CNS) and peripheral sensory organs use a variety of signaling molecules to perform diverse functions that allow animals to display complex and context-dependent behaviors. These functions, ranging from reception of sensory information to the integration of external environmental cues with the internal physiological state, dictate decisions made by the animal. To better understand how specific neuronal phenotypes within neural circuits are involved in sensory processing and social decisions, it is necessary to identify the transmitters expressed in different brain regions and sensory organs. Moreover, some signaling molecules act to modulate target neurons within a neural circuit, and this modulatory potential can change based on an animal's internal physiological conditions (Maruska & Butler, 2021). For example, sensory systems in females of many vertebrates often become more responsive to male courtship signals when in breeding conditions (e.g., during estrous or when gravid) compared to when they are not prepared to reproduce (Butler et al., 2019; Navarrete-Palacios et al., 2003; Sisneros & Bass, 2003). This correlated plasticity of the sensory and reproductive systems is due in part to the activities of different signaling molecules within the CNS; understanding how these molecules change with reproductive and social state can provide insights into their role in circuit function and evolution (Grone & Maruska, 2015; Grone et al., 2021; Whitaker et al., 2011).

One important signaling molecule used across vertebrates is nitric oxide (NO), a gaseous free radical that contributes to many biological functions throughout the body, including in the central and peripheral nervous systems. NO is produced during the conversion of L-arginine to L-citrulline by different isoforms of the enzyme nitric oxide synthase (NOS) (Alderton et al., 2001). NO functions as both a neurotransmitter and neuromodulator, often acting as a retrograde transmitter at synapses. In the nervous system, the expression of neuronal nitric oxide synthase (nNOS) is associated with both sensory and cognitive functionality. For example, genetic knockouts of nNOS in mice impair spatial learning, associative learning, and social recognition compared to wild-type mice (Jüch et al., 2009; Kelley et al., 2009; Kirchner et al., 2004), and impairment of nNOS synthesis disrupts olfactory learning (Pavesi et al., 2013). These effects may be related to NO activity in regions such as the hippocampus, prefrontal cortex, and olfactory bulbs (OBs) (Jüch et al., 2009; Kirchner et al., 2004; Zoubovsky et al., 2011). NO and nnos are also detected in tissues of multiple peripheral sensory organs, including visual (Vielma et al., 2012), auditory (Fessenden et al., 1999; Takumida & Anniko, 2002), olfactory (Kishimoto et al., 1993; Sülz et al., 2009), taste (Ambe et al., 2016; Zaccone, 2002), and tactile organs (Yonehara et al., 2003). In addition to effects on blood flow in these systems, NO functions as a neurotransmitter, contributing to the sensitivity, responsiveness, and adaptation of sensory neurons. Such findings emphasize the widespread contributions of NO in the brain and sensory processing.

NO is also an important signaling molecule for reproductive processes. In mammals, NO produced by non-neuronal tissues modulates the release of pituitary and gonadal hormones (e.g., luteinizing hormone and estradiol). In the central nervous system, nNOS-produced

NO is involved in the hypothalamic–pituitary–gonadal axis, stimulating the release of gonadotropin-releasing hormone, neuropeptide Y, and prostaglandins from the hypothalamus and both luteinizing and follicle-stimulating hormone from the pituitary (reviewed in Dixit & Parvizi, 2001). Genetic knockouts of nnos in mice show altered aggressive and sexual behaviors (Nelson et al., 1995; Trainor et al., 2007). Furthermore, nnos is expressed in cells that produce kisspeptin in the preoptic area (POA) and the arcuate nucleus (ARC) of prepubescent sheep (Bedenbaugh, 2018). In female mice, nNOS-immunoreactive neurons are known to change throughout the estrous cycle, with different nuclei involved in reproduction showing distinct patterns of expression over the span of the cycle (Sica et al., 2009). Although variation in the activity and expression of nnos has been reported across reproductive conditions of some mammalian model species, little is known about how this enzyme contributes to the sensory and neural plasticity of reproductive conditions in other vertebrates.

Teleosts are the most speciose group of vertebrates and display remarkably diverse social and reproductive behaviors, making them excellent models for examining the function and evolution of different signaling molecules. Here, we investigate the role of NO by examining the localization of nnos in the brain and sensory organs of the African cichlid fish Astatotilapia burtoni. This species of maternal mouthbrooding fish is an emerging model of neurobiological systems particularly amenable to comparing neural functioning and plasticity across reproductive conditions (Maruska & Fernald, 2018). Sexually mature females exhibit maternal care of their developing young and thus exist in multiple reproductive states. Ova develop in gravid females until ovulation, where the eggs are released from follicles prior to spawning. After fertilization, the female broods the eggs within her mouth. Brooding is a particularly energetically costly state, as females are unable to feed during the 2-week period while the offspring develop. Sexually mature males assume either dominant or subordinate phenotypes based on interactions with other males within the dominance hierarchy, and this status is liable to change depending on the social environment. Brightly colored dominant males, which accrue their status through triumphing over other males during intraspecific competition, defend territories and court females through visual, chemosensory, and acoustic displays (Butler et al., 2019; Field et al., 2018; Maruska & Butler, 2021; Maruska & Fernald, 2018; Maruska et al., 2012). Drab-colored subordinate males that were defeated during social interactions do not defend territories are reproductively suppressed and rarely court females. Previous studies in A. burtoni show reproductive state and social status plasticity in sensory function and the expression levels of several CNS signaling molecules in both males and females, but the distribution and plasticity of NO signaling is unknown (Butler & Maruska, 2019; Grone & Maruska, 2015; Grone et al., 2021; Maruska et al., 2017; Maruska, Butler, Field, et al., 2020; Porter et al., 2017).

Using in situ hybridization (ISH), we mapped the distribution of nnos-expressing cells throughout the brain, as well as in the retina and olfactory system of A. burtoni. We also quantified the expression of nnos across different reproductive conditions of both males (eyes, OBs) and females (eyes) in these tissues using quantitative PCR (qPCR). Our findings provide insights into the widespread role of NO signaling in the

CNS, retina, and olfactory system to support diverse functions in this cichlid species.

## 2 | MATERIALS AND METHODS

### 2.1 | Animals and tissue collection

Adult African cichlid fish *A. burtoni* (Günther, 1894) from a laboratory bred population were maintained in mixed-sex groups in flow-through 30 L aquaria under conditions similar to their native Lake Tanganyika (pH 8.0, 28–30°C, 300–500 µS cm⁻¹, 12L:12D light cycle, constant aeration). Aquaria contained gravel-covered bottoms and several halved terra cotta pots to serve as shelters and spawning territories. Fish were fed cichlid flakes daily (Aquadine, Healdsburg, CA, USA) and supplemented with brine shrimp several times a week. All experiments were performed in accordance with the recommendations and guidelines provided by the National Institutes of Health Guide for the Care and Use of Laboratory Animals, 2011. The protocol was approved by the Institutional Animal Care and Use Committee (IACUC protocol #18-101) at Louisiana State University, Baton Rouge, LA.

Fish were quickly netted from aquaria and measured for standard length (SL) and body mass (BM), immobilized in ice-cold cichlid-system water, and sacrificed by rapid cervical transection. Gonads were removed and weighed to calculate the gonadosomatic index [GSI = (gonad mass/BM) × 100] as a measure of reproductive investment. For in situ hybridization, brains were exposed, eyes were loosened from surrounding tissue, and entire heads were fixed at 4°C overnight in 4% paraformaldehyde (PFA) made in 1× phosphate-buffered saline (PBS), rinsed in 1×PBS, and cryoprotected in 30% sucrose prepared in 1×PBS for 1–2 days at 4°C. Brains and eyes (lens removed) were then dissected from the head and mounted in OCT media, sectioned in the transverse plane at 20 µm with a cryostat, and collected onto two alternate sets of charged slides (VWR Superfrost plus). Olfactory epithelia (OE) were immediately dissected out and fixed in 4% PFA for 30 min–1 h and then processed as above for brains and eyes. Slides were dried flat at room temperature for 2 days and stored at −80°C until staining.

For qPCR experiments, OBs and eyes (excess surrounding tissue and lens excluded) were removed after sacrifice and immediately frozen at −80°C prior to RNA isolations. Tissues were collected at the same time of day to minimize any potential diurnal variations in gene expression. Eye tissue samples were identical to those used in Butler et al. (2019). We examined gravid, ovulated, and mouthbrooding females, as well as dominant and subordinate males. OB tissue samples were collected from a different group of animals, and we compared dominant and subordinate males but did not quantify *nnos* in the OBs of female cichlids.

### 2.2 | Chromogenic in situ hybridization

To map the distribution of *nnos*-expressing cells in the brain, eye, and OE, we performed ISH in the brain for a total of eight males and four females and eyes in eight males and six females. All individuals were of mixed reproductive states. Although OE from multiple males and females were collected, our ISH did not label any *nnos*-expressing cells in this tissue, even after long development times (e.g., 18–22 h). In the brain and eye, our goal was to provide a complete distribution map of *nnos*-expressing cells based on consensus from fish of different sexes and reproductive conditions. Thus, only qualitative, not quantitative, differences were examined via ISH staining experiments. ISH was performed as previously described (Butler & Maruska, 2016; Grone & Maruska, 2015; Porter et al., 2017). Briefly, digoxigenin (DIG)-labeled riboprobes were made from whole-brain cDNA with commercially synthesized (Invitrogen) gene-specific primers and purified: forward 5′-GTACATGGGCACAGAGATTG-3′, reverse 5′-TCCGAGTGTCAGAGTAAGAG-3′; 806 bp product. Antisense primers had the T3 RNA polymerase promotor sequence added to the reverse primer (aattaaccctcactaaaggg). Sense control probes were generated in the same manner but had the T3 RNA polymerase promoter sequence added to the forward primer. Slides of cryosectioned tissue were brought to room temperature, and the tissue was surrounded with a hydrophobic barrier (Immedge pen, Vector Laboratories). The tissue was treated with the following solutions: 1×PBS (3 × 5 min), 4% PFA (20 min), 1×PBS (2 × 5 min), proteinase K (10 min), 1×PBS (10 min), 4% PFA (15 min), 1×PBS (2 × 5 min), Milli-Q water (3 min), and 0.1 M triethanolamine-HCl pH 8.0 with acetic anhydride (10 min)1×PBS (5 min). The issue was then prehybridized for 3 h in a sealed chamber at 60–65°C, followed by incubation with DIG-labeled probe solution. Slides with DIG-labeled probe were covered with hybrislips and hybridized overnight (∼18 h) in a 60–65°C oven. After hybridization, stringency washes were performed first at 60°C as follows: 2× saline sodium citrate (SSC): 50% formamide (2 × 30 min), 1:1 mixture of 2× SSC: maleate acid buffered with Tween-20 (MABT; 2 × 15 min), and MABT (2 × 10 min). Slides were then transferred to room temperature and washed with MABT (2 × 10 min), followed by blocking of nonspecific binding with MABT containing 2% bovine serum albumin (BSA) for 3 h at room temperature. After blocking, slides were incubated with anti-DIG alkaline phosphatase (AP) antibody (Roche Cat# 11093274910, RRID: AB_514497; diluted 1:5000 in blocking solution) overnight at 4°C in a sealed humidified chamber. Slides were then washed in MABT (3 × 30 min), treated with AP buffer (2 × 5 min) and developed in NBT/BCIP solution at 37°C (brain, 4 h; retina and OE, 18–22 h). Following development, slides were treated with 1×PBS (3 × 5 min), 4% PFA (10 min), and 1×PBS (3 × 5 min). Slides were coverslipped with aqueous mounting media (Aquamount, Lerner Laboratories), dried flat overnight, and then had their edges sealed with clear nail polish.

### 2.3 | Imaging and analysis

To map the distribution of *nnos*-expressing cells in the brain and eye, slides of stained tissue were visualized on a Nikon Eclipse Ni microscope controlled by Nikon Elements software (RRID:SCR_014329), and photographs were taken with a color digital camera (Nikon DS-Fi2).

Localization results are based on consensus staining from all animals (mixed sex and reproductive states), as we were not able to see appreciable differences in staining distributions among individuals of different sexes or reproductive conditions. Images were adjusted for contrast, brightness, and levels as needed in Photoshop (Adobe Systems, San Jose, CA, USA; RRID: SCR_014199). Distracting artifacts were removed with the Photoshop clone tool as needed. To facilitate the identification of neuroanatomical structures and brain nuclei, we used a cresyl violet-stained *A. burtoni* reference brain and annotated atlas, as well as other brain atlases from this and other teleost species (Burmeister et al., 2009; Maruska et al., 2017; Maruska, Butler, Anselmo, et al., 2020; Muñoz-Cueto, 2001; Wullimann et al., 1996).

## 2.4 | Expression of *nnos* in the brain and sensory organs

To determine which brain regions and peripheral sensory organs express the *nnos* transcripts, we used macrodissections, RT-PCR, and gel electrophoresis. For brain regions, we carefully dissected and removed brains from adult dominant males. The pituitary and OBs were first removed and collected separately. Next, the telencephalon was separated just rostral to the optic nerves using a surgical blade to ensure that the preoptic area remained with the hypothalamus. The hypothalamus was separated just below the midbrain, and the hindbrain portion was separated just caudal to the tectum. The resulting midbrain portion also contains some thalamic nuclei. The spinal cord was severed just proximal to the medulla, and the corpus cerebelli was separated at the most ventral portion where it reached the medulla oblongata. For sensory tissues, whole eyes with lenses removed, both rosettes that comprise the olfactory epithelia, and both saccules of the inner ear (largest auditory endorgan in teleosts) were collected. All samples were immediately frozen and stored at −80°C until RNA isolation.

Macrodissected brain regions and sensory organs were homogenized, RNA was isolated using RNeasy Plus Micro or Mini kits (Qiagen; Germantown, MD, USA) following the manufacturer's protocols, and RNA was reverse transcribed to cDNA using qScript (Quantabio). cDNA, Platinum PCR 2× SuperMix (ThermoFisher), nuclease-free water, and gene-specific primers were combined for PCR (95°C for 1 min; 40 cycles of 95°C for 30 s, 55°C for 30 s, 72°C for 1 min; 72°C for 1 min). The following primers were commercially synthesized (Invitrogen): forward 5′-AGCCTCGCTACTATTCTATCA-3′; reverse 5′-ATTGGTCCCTCTCCATCTC-3′; 106 bp product). Approximately 4 μl of PCR product and 2 μl of loading dye were loaded into each well and run on a 2% agarose gel (1×TBE) with GelRed at 65 V for 45–60 min. The products were visualized on a Bio-Rad ChemiDoc Imaging system and verified to be the appropriate size in relation to the ladder (100 bp TrackIT). In addition, all samples were run with β-actin as a positive control. Negative controls (no RT enzyme in RT-PCR and no cDNA template in PCR) showed no bands in any reactions. PCR products were sequenced (Eurofin Genomics, Louisville, KY, USA) for verification of primer specificity and correct amplification of the *nnos* target gene.

## 2.5 | Quantitative PCR

To test for sex, reproductive condition, and social status plasticity in *nnos* expression in sensory tissues of the eye and OB, tissue was homogenized, and RNA was extracted following the manufacturer's protocol (RNeasy Plus Mini Kit–eyes, RNeasy Plus Micro Kit–OEs; Qiagen). RNA yields were calculated using spectrophotometric values to ensure consistent RNA inputs to cDNA synthesis reactions (qScript, QuantaBio). PerfeCTa SYBR Green Fastmix (Quantabio) was used for qRT-PCRs with gene-specific primers. We measured the levels of *nnos* using the following commercially synthesized (Invitrogen) primers designed from the *A. burtoni* sequence in NCBI GenBank (XM_005928872.2): forward 5′-AGCCTCGCTACTATTCTATCA-3′; reverse 5′-ATTGGTCCCTCTCCATCTC-3′ (106 bp product). Primers for the reference genes *gapdh*, *18s*, and *eef1a* were also commercially synthesized (Invitrogen) and validated previously (Butler et al., 2019; Maruska & Fernald, 2010a, 2010b; Porter et al., 2017). Each primer pair had a single melt curve peak, amplified in a positive control (brain cDNA), and showed no amplification in no-RT negative controls. The amplified *nnos* product was also verified to produce a single band of the correct size using 1% agarose gel electrophoresis and commercially sequenced (Eurofins Genomics) to verify amplification of the correct *nnos* gene.

qPCR was performed on a CFX Connect Real-Time system (BioRad) with duplicate 20 μl reaction volumes. The cycling parameters were 95°C for 30 s, 45 cycles of 95°C for 1 s, and 60°C for 15 s, followed by a melt curve analysis. Fluorescence thresholds for each sample were automatically measured (CFX Manager, BioRad), and PCR Miner (Zhao & Fernald, 2005) was used to calculate reaction efficiencies and cycle thresholds for each individual well. The relative amount of *nnos* mRNA in each sample was normalized to the geometric mean of two different reference genes for each tissue (eyes, *eef1a* and *gapdh*; OB, *gapdh* and *18s*) as follows: relative target gene mRNA levels = $[1/(1 + E_{target})^{CTtarget}]/ [1/(1 + E_{geomean})^{CTgeomean}] \times 100$, where $E$ is the reaction efficiency and CT is the average cycle threshold of the duplicate wells. Different reference genes were used in OB and eyes because qPCR experiments occurred at different times, and while several reference genes were tested in each tissue, we used those that were verified to not differ among our compared groups ($p > .05$), indicating that they are appropriate for the study.

## 2.6 | Statistical analyses

Data from qPCR were analyzed in R (R Core Team, 2021). Relative *nnos* expression data were fit to linear models, using status (dominant and subordinate for males; ovulated, gravid, and brooding for females) as the sole factor. Comparisons among multiple groups were performed with preplanned orthogonal contrasts via the contrastmeans function of the predictmeans package (Luo et al., 2018). We compared males and females, dominant and subordinate males, ovulated and gravid females, and brooding females against ovulated and gravid females together.
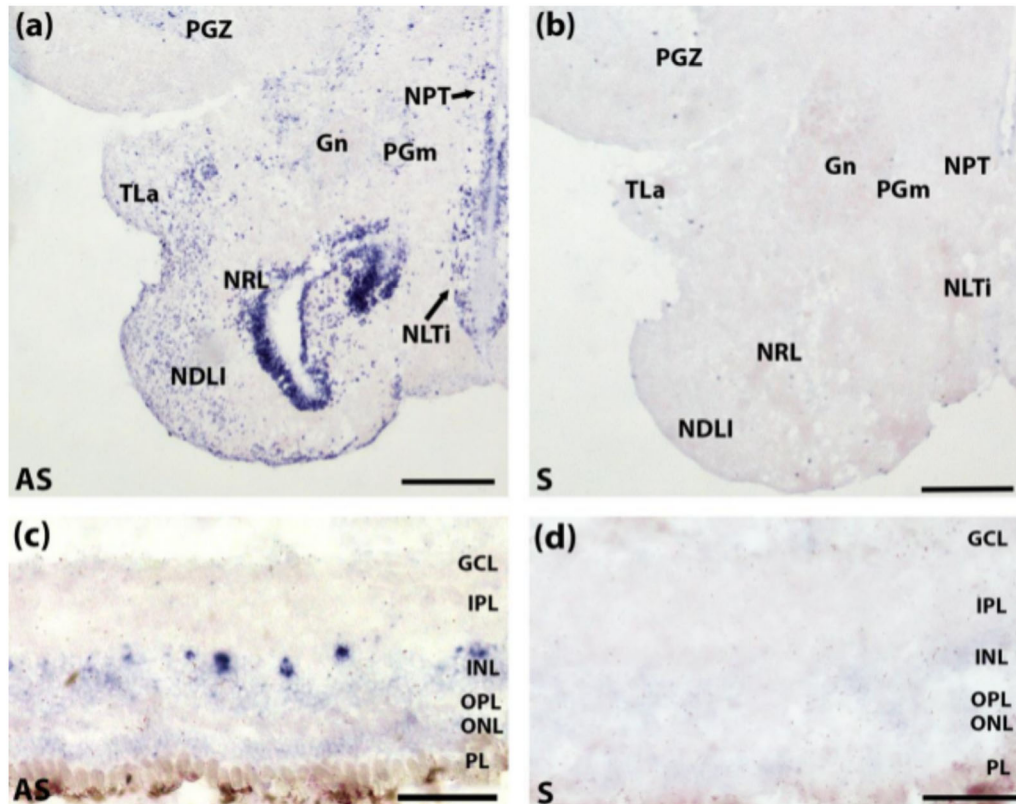
**FIGURE 1** Representative examples of chromogenic in situ hybridization (ISH) staining in the brain and retina of *A. burtoni* to show *nnos* probe specificity. Antisense (AS; a and c) and sense (S; b and d) control probes are shown. Photomicrographs were taken on alternate 20 μm transverse sections from the same brain and retina run simultaneously in the same ISH experiment. The sense control probe did not show positive staining (b and d). See list for abbreviations. Scale bars = 250 μm (a and b); 25 μm (c and d)

## 3 | RESULTS

To localize regions of *nnos* expression throughout the *A. burtoni* brain and retina, we used chromogenic ISH with riboprobes on males and females of different reproductive and social states (GSI mean ± *SD* = dominant males: 0.58 ± 0.40; subordinate males: 0.21 ± 0.06; females (all conditions): 3.14 ± 3.55. SL (mm) mean ± *SD* = dominant males: 43.57 ± 7.07; subordinate males: 39.00 ± 8.04; females (all conditions): 37.43 ± 7.57. BM (g) Mean ± *SD* = dominant males 2.55 ± 1.32; subordinate males 1.70 ± 0.85; females (all conditions) 1.37 ± 0.84). Tissue treated with antisense ISH DIG-labeled probes showed positive *nnos* staining throughout the brain and retina, while tissue treated with sense control probes showed no staining (Figure 1). ISH of the olfactory epithelium from multiple individuals never revealed any positive *nnos* staining.

### 3.1 | Localization of *nnos* expression in the brain

#### 3.1.1 | OBs and telencephalon

Expression of *nnos* in the OBs occurred as scattered cells only within the inner cellular layer (ICL, Figures 2a, 3a, and 4a). In the telencephalon, *nnos* was expressed in multiple dorsal (pallial) and ventral (subpallial) nuclei. Staining occurred along the midline in subdivision 1 of the medial part of the dorsal telencephalon (Dm-1) in rostral sections, and some scattered cells were found along the ventral portion of subdivision 3 (Dm-3). Cells were abundant within the central part of the dorsal telencephalon in subdivisions 4 (Dc-4) and 5 (Dc-5) but were fewer and more scattered in Dc-1, Dc-2, and Dc-3 (Figures 2b–f, 3b,c, and 4a–c). Stained cells were present within subdivisions 1 and 2 of the ventral zone of the lateral zone of the dorsal telencephalon (Dl-v1, Dl-v2), dorsal (Dd-d) and ventral (Dd-v) subdivisions of the dorsal part of the dorsal telencephalon, and the granular zone of the lateral zone of the dorsal telencephalon (Dl-g) (Figures 2b,d,e, 3a,b, and 4a–c). Some cells were also found along the lateral outer edge of the dorsal part of the dorsal telencephalon in more caudal sections (Dd), and stained cells were dense in the posterior part of the dorsal telencephalon (Dp) (Figure 2f). In the subpallium, *nnos*-expressing cells occurred in the medial area of the rostral subdivision of the dorsal part of the ventral telencephalon (Vd-r), becoming progressively more lateral in position approaching the posterior of this nucleus. Stained cells also occurred throughout the medial part of the supracommissural nucleus of the ventral telencephalon (Vs-m), the ventral nucleus of the ventral telencephalon (Vv), the lateral part of the ventral telencephalon (Vl), the intermediate nucleus of the ventral telencephalon (Vi), the central nucleus of the ventral telencephalon (Vc), the postcommissural nucleus of the ventral telencephalon (Vp), and the caudal subdivision
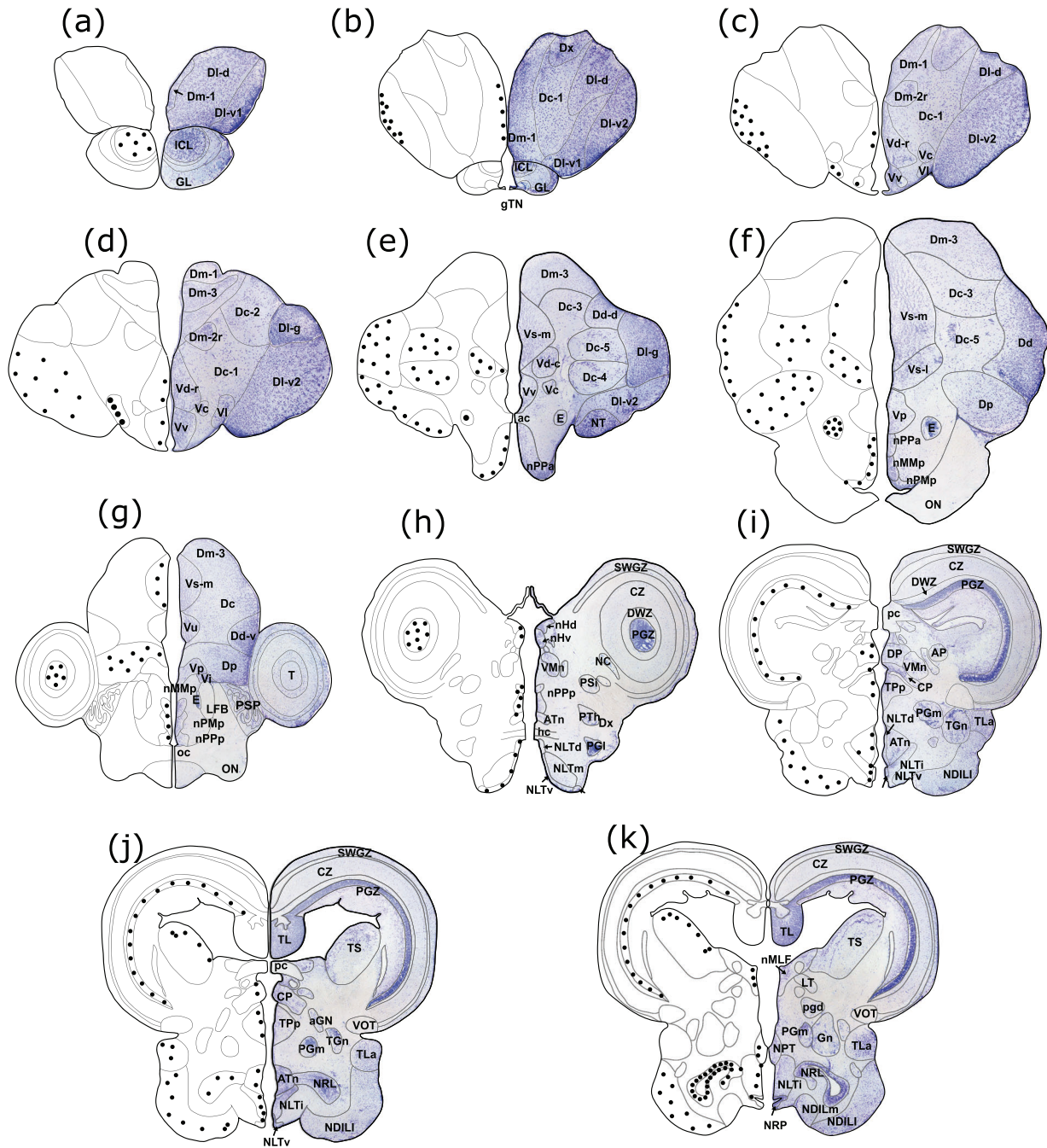
**FIGURE 2** Summary of the localization of *nnos*-expressing cells throughout the brain of *A. burtoni*. Representative transverse sections are shown from rostral (a) to caudal (v). Each shows a transverse section stained with cresyl violet, with nuclei and other neuroanatomical structures labeled (right side) and a traced mirror image (left side). Localization of cells (dots) expressing *nnos* are shown on traced images of the left side of each transverse section. See list for abbreviations

of the dorsal part of the ventral telencephalon (Vd-c) (Figures 2c–g, 3b, and 4b,c).

### 3.1.2 | Diencephalon

In the diencephalon, *nnos*-expressing cells occurred throughout the preoptic area (POA). Stained cells were located in the anterior part of the parvocellular preoptic nucleus (nPPa), the magnocellular

division (nMMp) and parvocellular divisions (nPMp) of the magnocellular preoptic nucleus, and the posterior part of the parvocellular preoptic nucleus (nPPp) (Figures 2e,f and 3d). Cells also lie in the entopeduncular nucleus (E).

In the thalamic region, *nnos*-expressing cells appeared in the accessory pretectal nucleus (APn), central (CP) and dorsal (DP) posterior thalamic nuclei, ventromedial thalamic nucleus (VMn), dorsal and ventral habenular nucleus (nHd/v) and lateral nucleus of the torus lateralis
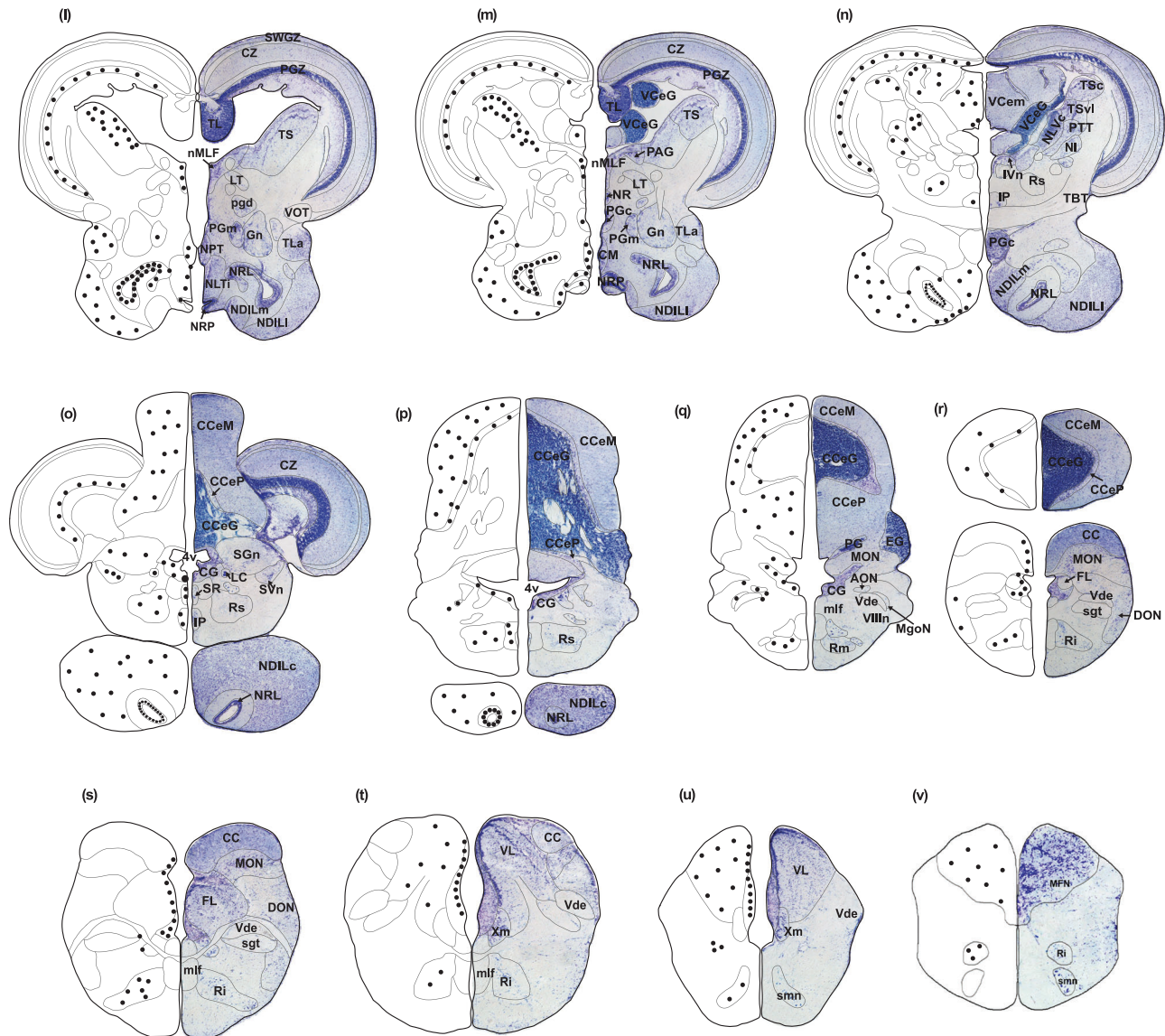
**FIGURE 2** Continued

(TLa) (Figures 2g–j, 3d,e, and 4d). A medial band of stained cells occurred throughout the commissural preglomerular nucleus (PGc). Stained cells also occurred in the anterior tuberal nucleus (ATn), posterior tuberal nucleus (NPT), and dorsal (NLTd), intermediate (NLTi), and ventral (NLTv) areas of the lateral tuberal nuclei (Figures 2h–l, 3d–e, and 4d). Scattered cells also lie along the midline in the region of the periventricular nucleus of the posterior tuberculum (TPp) (Figures 2i, 3e, and 4e). The lateral (PGl) and medial (PGm) preglomerular nuclei also contained *nnos*-expressing cells. In the hypothalamic region, stained cells were detected in the medial (NDILm) and lateral (NDILl) parts of the diffuse nucleus of the inferior lobe (Figures 2i–n, 3f,g, and 4d–f). Cells are also found in the dorsal (PPd) and ventral (PPv) periventricular pretectal nuclei and the intermediate (PSi), lateral (PSl), and medial (PSm) divisions of the superficial pretectal nuclei (Figures 2h, 3e, and 4d). Cells also occurred along the ventral and medial borders of the caudal part of the diffuse nucleus of

the inferior lobe (NDILc). Dense cellular expression occurred in the lateral (NRL) and posterior recess (NRP) nuclei (Figures 2k–p, 3g, and 4e–g). Several large cells also lie within the nucleus of the medial longitudinal fasciculus (nMLF) along the midline beneath the ventricle (Figure 2k–m). Stained cells were scattered in the corpus mammillare (CM) (Figure 2m). Staining was not observed in the pituitary gland.

### 3.1.3 | Mesencephalon and rhombencephalon

In the midbrain, *nnos*-expressing cells occurred in the periventricular gray zone (PGZ) of the tectum throughout its rostral-caudal length but were more abundant in the caudal PGZ (Figures 2h–o, 3h, and 4d–g). Stained cells were found in the caudal (TSc) and ventrolateral (TSvl) nuclei of the torus semicircularis (TS) (Figures 2j–n, 3f, and 4e,f,g). Cells also lie in the paratoral tegmental nucleus (PTT).
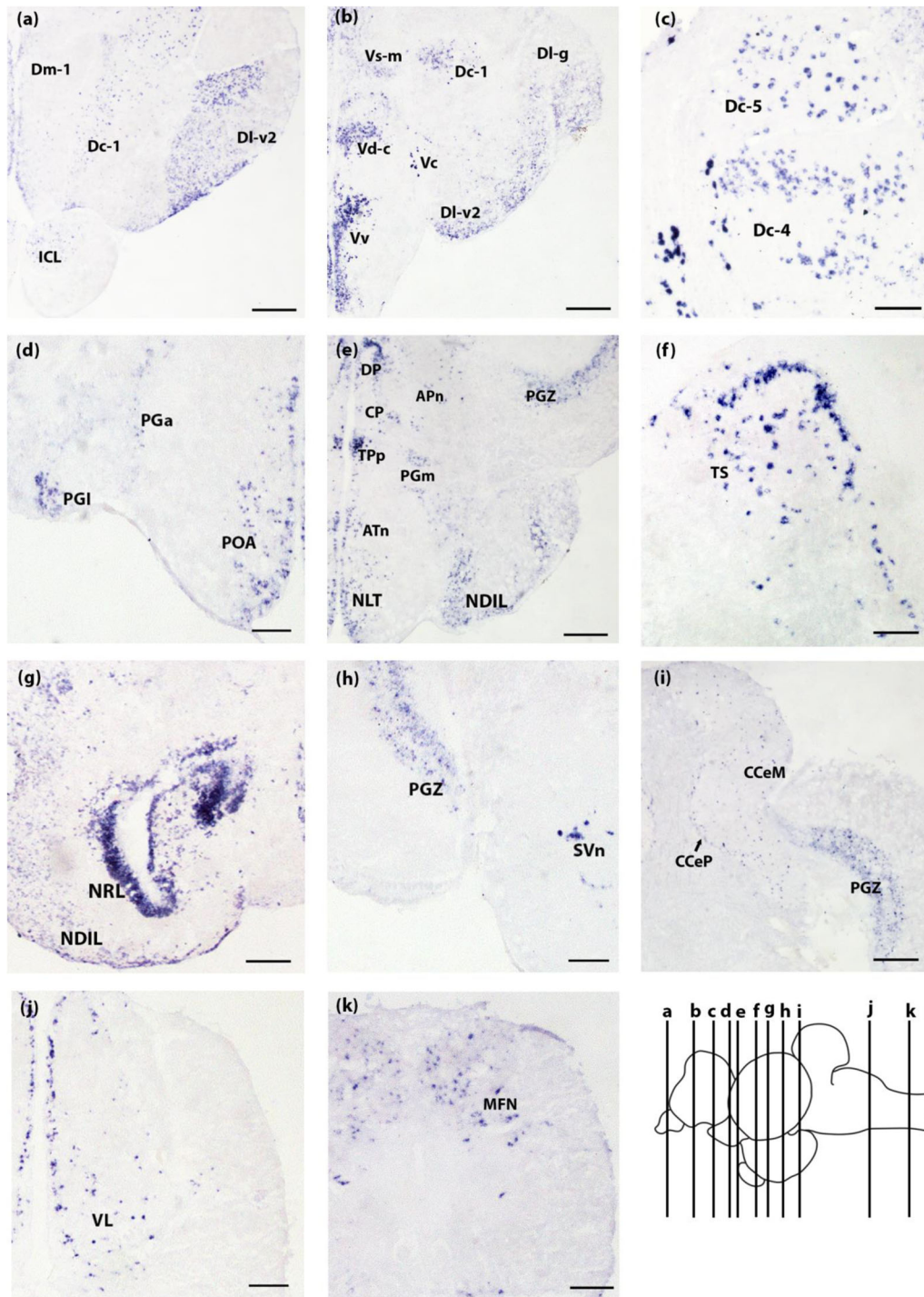
**FIGURE 3** Representative photomicrographs of *nnos*-expressing cells in the brain of *A. burtoni*. *nnos*-expressing cells are found in the inner cellular layer of the olfactory bulb and in various nuclei of the dorsal telencephalon (a). Densely stained cell populations are found in many nuclei of the ventral telencephalon (b). A population of *nnos*-containing cells is found in the central dorsal telencephalon (c). The preoptic area and nucleus prethalamicus contain stained cells (d). *nnos*-expressing cells are found in the thalamic nuclei and in several midbrain regions (e). Scattered *nnos*-expressing cells are found in the torus semicircularis (f). Densely stained cell populations are shown in the nucleus of the lateral recess and the medial nucleus of the inferior lobe, while more scattered cells are found in the diffuse nucleus of the inferior lobe (g). The periventricular gray zone of the tectum and the secondary visceral nucleus both contain *nnos*-expressing cell populations (h). Several regions of the cerebellum contain *nnos*-expressing cells (i). Scattered cells are found in the vagal lobe and the central gray along the border with the fourth ventricle (j). *nnos*-containing cells are present in the medial funicular nucleus (k). Photomicrographs were taken from 20 μm transverse sections. Scale bars = 250 μm (a, b, e, and i); 100 μm (c and f); 125 μm (d, g, h, j, and k). The inset of the sagittal brain at the bottom right shows the approximate locations of each transverse section. See list for abbreviations
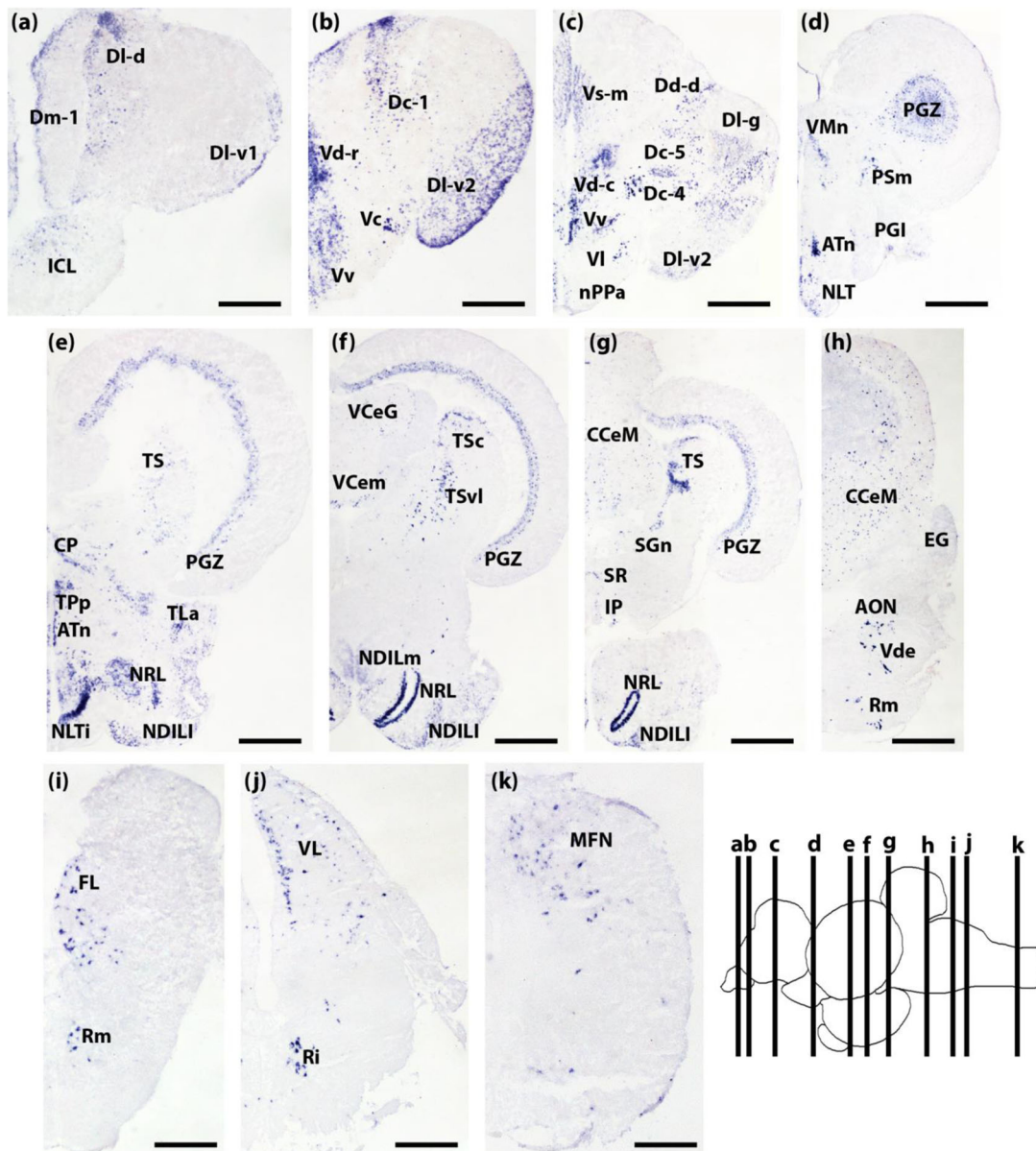
**FIGURE 4** Representative photomicrographs of *nnos*-containing cells throughout *A. burtoni* at lower magnification. The internal cellular layer of the olfactory bulb contains *nnos*-expressing cells (a). *nnos*-containing cells are found in the nuclei of the dorsal and ventral telencephalon (b and c). Expression of *nnos* is found throughout the midbrain and thalamic regions (d, e, and f). Granular, molecular, and Purkinje layers of the cerebellum contain *nnos*-expressing cells (g, h). *nnos*-containing cells are found in several nuclei of the hindbrain (I, j, and k). Photomicrographs were taken from 20 μm transverse sections. Scale bars = 250 μm. The inset of the sagittal brain at the bottom right shows the approximate locations of each transverse section. See list for abbreviations

In the rhombencephalon, *nnos*-expressing cells occurred in the molecular layer of the valvular cerebelli (VCeM) (Figures 2n and 4f). Anterior staining of the molecular layer of corpus cerebelli (CCeM) gives rise to a more scattered distribution of stained cells caudally, with a less dense distribution of stained cells in the granular layer of corpus cerebelli (CCeG) (Figures 2o–r, 3i, and 4g,h). In the caudal corpus cerebelli, a few cells also lie in the Purkinje layer (CCeP) (Figures 2o–r and 3i). Some cells were also observed in the secondary visceral nucleus (SVn) and secondary gustatory nucleus (SGn) and along the medial border of the isthmal nucleus (NI) (Figures 2n–o, 3h,

and 4g). More caudally, stained cells were found in the interpeduncular nucleus (IP) along the ventral midline, in the locus coeruleus (LC), and in the superior raphe nucleus (SR) (Figures 2o and 4g). Scattered cells also lie within several octavolateralis nuclei, such as dorsal (DON), anterior (AON), and magnocellular (MgON) octaval nuclei, as well as in the facial lobe (FL) (Figures 2r–s and 4h–i). *nnos*-expressing cells occurred throughout the sensory region of the vagal lobe (VL) (Figures 2s–u, 3j, and 4i,j). Staining was consistently present in the central gray (CG) surrounding the fourth ventricle from the midbrain regions into the hindbrain (Figure 2o–p). A few large cells were also stained in the
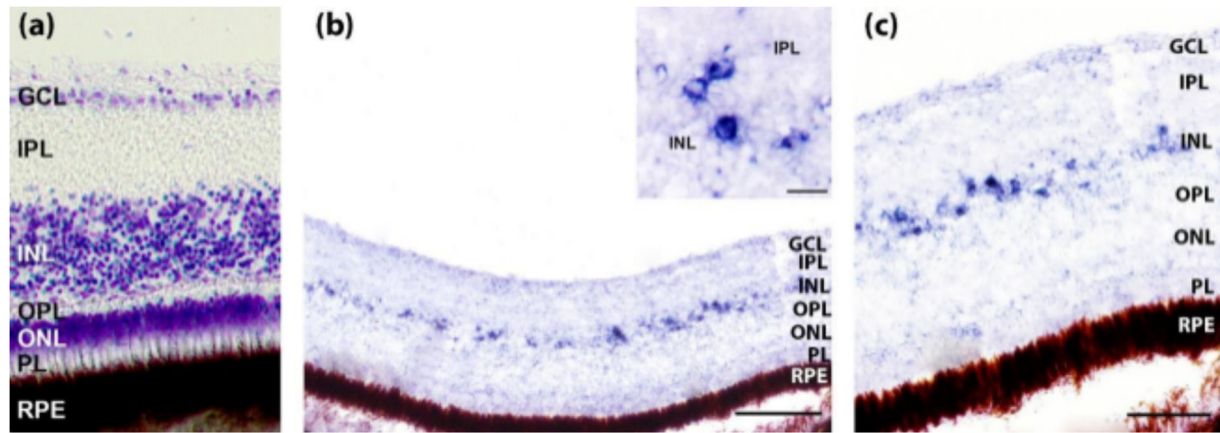
**FIGURE 5** Representative photomicrographs of *nnos*-containing cells in the retina of *A. burtoni*. Layers of the retina are shown by cresyl violet staining for reference (a). *nnos*-expressing cells are present in the inner nuclear layer (INL) of the retina at the border of the inner plexiform layer (IPL) (b and c). The inset in (b) shows a higher magnification of several *nnos*-expressing cells in the INL. Photomicrographs were taken from 20 µm transverse sections of a dominant male cichlid. Scale bars = 100 µm (b), 10 µm (b inset), 50 µm (c). See list for abbreviations

reticular nuclei, including the inferior (Ri), middle (Rm), and superior (Rs) reticular nuclei (Figures 2p–t,v and 4i,j). Staining was also seen near these nuclei and may include cells of the spinal motor neurons (smn) (Figure 2u). Abundant *nnos*-expressing cells also lie in the medial funicular nucleus (MFN) (Figures 2v, 3k, and 4k) and commissural nucleus of Cajal (NCC) in the caudal medulla (not shown).

## 3.2 | Localization of *nnos* expression in the eye

In the retina, *nnos*-expressing cells were abundant in the inner nuclear layer of the retina along the border with the inner plexiform layer but were absent from other layers (Figure 5). The location of these *nnos*-expressing cells suggests that they are a type of amacrine cell but this requires confirmation. The distribution of *nnos*-expressing cells in the retina appeared similar across both sexes and all reproductive conditions.

## 3.3 | Expression of *nnos* in the brain and sensory organs

We used RT-PCR and gel electrophoresis to localize transcripts of *nnos* in macrodissected brain regions and sensory organs (Figure 6). Expression of *nnos* was found in all brain regions but not in the pituitary gland. Strong bands were observed in the whole brain, telencephalon, hypothalamus, midbrain/thalamus, and cerebellum, with slightly fainter bands in the hindbrain and spinal cord and a weak band in the OBs. In sensory organs, *nnos* was detected in the eyes but not in the OE nor in the saccules of the inner ear (Figure 6).

## 3.4 | Quantification of *nnos* in the eyes and OBs

Because RT-PCR and ISH revealed *nnos* expression in retina and OBs, we used qPCR to quantify *nnos* mRNA levels in these tissues across

reproductive and social states (GSI mean $\pm$ *SD* = dominant males: 1.07 $\pm$ 0.23; subordinate males: 0.24 $\pm$ 0.14; gravid females: 9.23 $\pm$ 1.26; ovulated females: 7.48 $\pm$ 3.59; brooding females: 0.57 $\pm$ 0.22. SL (mm) mean $\pm$ *SD* = dominant males: 65.33 $\pm$ 3.67; subordinate males: 61.00 $\pm$ 5.02; gravid females: 37.13 $\pm$ 3.09; ovulated females: 38.83 $\pm$ 6.43; brooding females: 36.29 $\pm$ 4.61. BM (g) mean $\pm$ *SD* = dominant males 8.38 $\pm$ 1.29; subordinate males 6.23 $\pm$ 1.41; gravid females 1.80 $\pm$ 0.40; ovulated females 2.34 $\pm$ 0.66; brooding females 1.90 $\pm$ 1.00). We also performed qPCR on OE tissue, but similar to the ISH and RT-PCR results, we did not detect *nnos* mRNA in OE. In the eye, males expressed significantly more *nnos* than females (contrast of means $t_{53}$ = 4.66, *p* < .01), and dominant males had greater *nnos* levels than subordinate males (contrast of means $t_{53}$ = 2.19, *p* < .05; Figure 7a). Although ovulated females had the highest mean *nnos* expression in the eye, differences among female reproductive states were not significantly different.

In the OBs, dominant males had greater *nnos* mRNA levels than subordinate males (analysis of variance $F_{1,16}$ = 7.7467, *p* < .05; Figure 7b). We did not have OB tissue available for females to compare *nnos* levels across reproductive states in this study.

## 4 | DISCUSSION

We present the localization and quantification of the NO-producing enzyme *nnos* in the brain, eyes, and olfactory system of a social and reproductively plastic teleost fish. We further show that *nnos* in the eyes is greater in males than in females, and levels differ with male dominance status but not female reproductive state. Furthermore, *nnos* in the OBs of dominant males is greater than those of subordinate males. These data suggest diverse roles for gaseous NO signaling in both sexes, with a potential role of greater importance in mediating the sensory perception required for structuring male social hierarchies or male courtship.
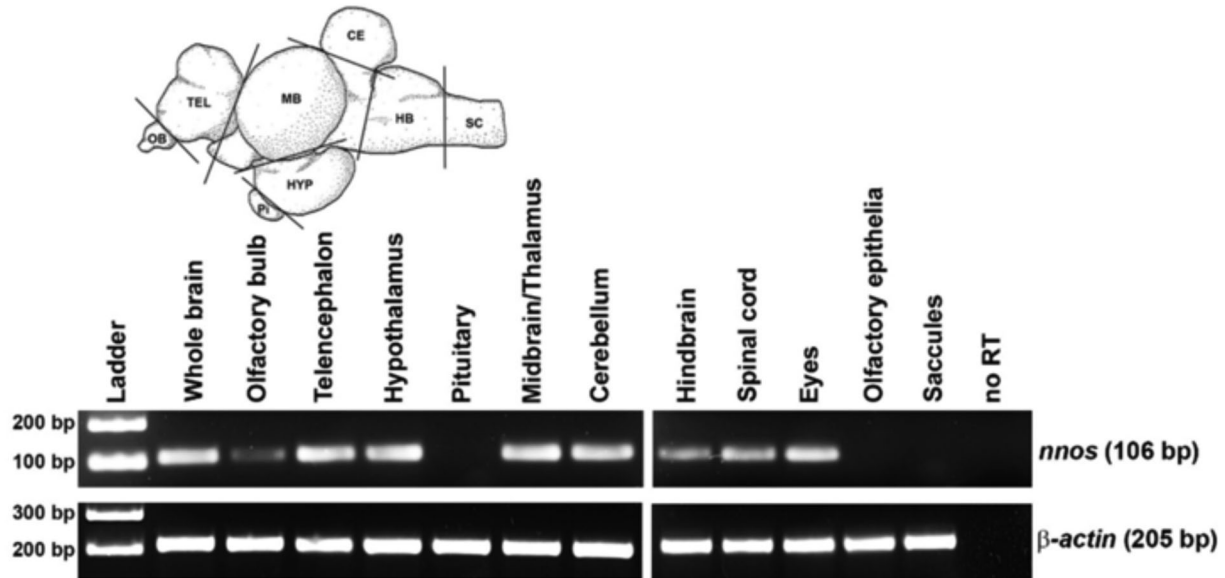
**FIGURE 6** Expression of *nnos* transcripts in macrodissected brain regions and sensory organs of adult *A. burtoni*. Representative tissue distribution of transcripts is shown by PCR and gel electrophoresis from reverse transcribed cDNA. PCR products from *β-actin* transcripts in the same samples are shown below. The inset shows a sagittal view of the *A. burtoni* brain to illustrate the approximate macrodissection cuts used for analysis. A nonreverse transcriptase (no RT) negative control and DNA ladder (100 bp ladder) are also shown. Base pair (bp) numbers to the left are sizes of the indicated ladder bands, and bp numbers to the right are product sizes for *nnos* and *β-actin*. The levels, contrast, and brightness of the gel images were adjusted in Photoshop. Abbreviations: CE, cerebellum; HB, hindbrain; HYP, hypothalamus; MB, midbrain, and thalamus; OB, olfactory bulb; Pi, pituitary; SC, spinal cord; TEL, telencephalon
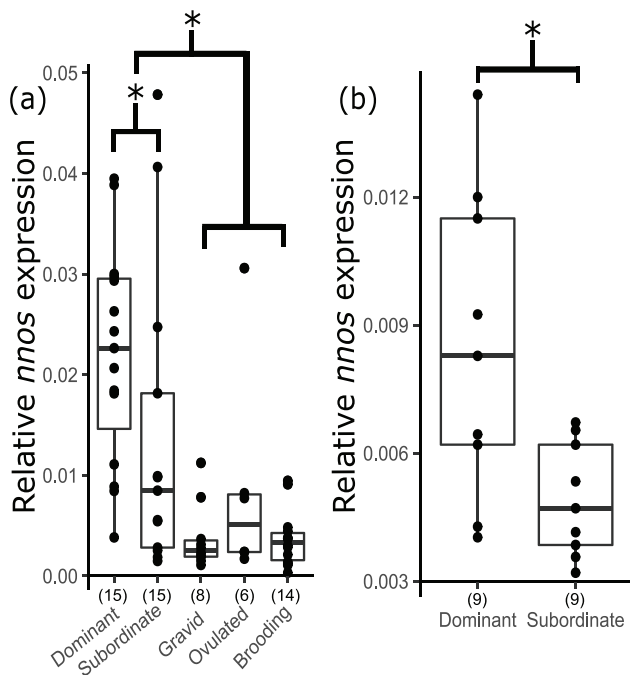


**FIGURE 7** Relative *nnos* expression in (a) the eyes of male and female *A. burtoni* of different reproductive states and (b) the olfactory bulbs of dominant and subordinate males. Filled circles show individual data points. Data are expressed as relative *nnos* mRNA levels normalized to the reference genes. Boxplots show the 25th and 75th percentiles, solid lines denote the median of data, and whisker lengths are 1.5 × interquartile range. Asterisks denote significant differences at $p < .05$ (contrasts of means/analysis of variance). Numbers in parentheses indicate the number of fish in each group

We chose to examine NO-producing cells via the detection of mRNA for the *nnos* enzyme because it is more specific than detection by antibodies or chemical molecules that are more prone to nonspecific labeling, but the literature on the localization of NO-producing cells in many vertebrates includes examinations through multiple methods. Importantly, these methods are not always congruent (Sánchez-Islas & León-Olea, 2001). For example, NADPH-diaphorase (NADPH-d) histochemistry is used widely as an indicator of nitrergic cells across taxa (Brüning & Mayer, 1996; González et al., 2002; Ota et al., 1999; Virgili et al., 2001). While NADPH-d staining corresponds to NOS immunoreactivity in the rat brain, it has misrepresented NOS in the olfactory system of salmon (Lema & Nevitt, 2001), suggesting that equating NADPH-d staining with nNOS presence should not be generalized across tissues or among species without performing proper controls. A previous study of NADPH-d in the brain of *A. burtoni* also failed to detect the molecule in many brain regions in which we report abundant *nnos* expression, such as in the POA (Jadhao & Malz, 2004). Different staining techniques may produce variable results due to differences in the amounts of target molecules produced or stored within cells, binding affinities of reagents, or even isoforms of genes from teleost genome duplication (Porter et al., 2017). Furthermore, many studies do not provide detailed descriptions or images of distribution patterns with high neuroanatomical resolution throughout the entire brain, making comparisons among species difficult and incomplete. Such discrepancies are worth noting, as we compared the distribution of *nnos* in *A. burtoni* by in situ hybridization, qPCR, and RT-PCR to that detected by other methods in other species.

## 4.1 | Distribution of *nnos* in the brain compared to other fishes and other vertebrates

PCR indicated that *nnos* was expressed in all major parts of the *A. burtoni* brain but not in the pituitary, and we found *nnos*-labeled cells with ISH in nuclei throughout these same brain regions, as in other teleosts (Biswas et al., 2015; Gaikwad et al., 2009; Giraldez-Perez et al., 2009; Holmqvist, 2004; Virgili et al., 2001). In *A. burtoni*, the OB was an area of relatively low *nnos* expression, with scattered cells found only in the ICL, and we discuss the potential relationships of *nnos* with olfactory behaviors below (Section 4.3). Although *nnos* expression is reported in the OBs of several species of fishes (Ferrando et al., 2012; Gaikwad et al., 2009; Lema & Nevitt, 2001; López et al., 2019; Virgili et al., 2001), studies have failed to detect *nnos* in more primitive fishes, such as gars and members of the subclass Cladistia (López et al., 2016, 2017). Thus, the role of NO signaling in the OBs may be a more recently derived trait within fishes.

Among teleosts, the distribution of *nnos*-expressing cells seems to be rather conserved, with a high degree of detection in the telencephalon and diencephalon and with reduced expression in more caudal brain regions (Bordieri et al., 2005), to which our results concur. We found *nnos* expression in many dorsal and ventral areas of the telencephalon, as in other fishes (Biswas et al., 2015; Gaikwad et al., 2009; Giraldez-Perez et al., 2009; Holmqvist et al., 2000; López et al., 2016, 2017; Masini et al., 2005; Virgili et al., 2001). Thus, NO signaling appears prevalent in both pallial and subpallial nuclei of the telencephalon across many fish species, suggesting diverse functions related to decision-making, cognition, sensory perception, and expression of behaviors.

For many fishes, *nnos* expression is reported throughout the diencephalon, notably in nuclei of the POA (Ando et al., 2004; Biswas et al., 2015; Gaikwad et al., 2009; Giraldez-Perez et al., 2009; Jadhao & Malz, 2003; López et al., 2016, 2017, 2019; Virgili et al., 2001). These studies also commonly report the presence of *nnos* in the thalamus, hypothalamus, and pineal and habenula, sites that are also stained in *A. burtoni*. Although we have no evidence for *nnos* expression in the pituitary of *A. burtoni*, nor in several other species of fishes examined, it was reported by immunostaining in the rostral pars distalis of the catfish (Gaikwad et al., 2009; Jadhao & Malz, 2003). The widespread *nnos* expression in hypothalamic and preoptic areas supports the existing evidence for NO signaling in the regulation of reproductive physiology via interactions with important neuropeptides in several taxa (Bordieri et al., 2005; Chang & Pemberton, 2018; Escobar et al., 2013; Grone et al., 2010; Maruska, Butler, Anselmo, et al., 2020; Maruska, Butler, Field, et al., 2020; Ohga et al., 2018). Further study of the interactions of NO and other gene products in specific regions of the brain may highlight important mechanisms underpinning the evolution of vertebrate neuroendocrine systems.

In the mesencephalon, *nnos* is expressed throughout the tectum in multiple fish species (Ando et al., 2004; Giraldez-Perez et al., 2009; Holmqvist et al., 2000; López et al., 2019; Masini et al., 2005; Virgili et al., 2001). We found *nnos* only in the PGZ, as is common in teleosts, but other species express *nnos* in additional tectal layers (Gaikwad

et al., 2009; Giraldez-Perez et al., 2009). As in *A. burtoni*, *nnos* is detected in the TS and TLa of several species (López et al., 2016, 2017, 2019; Masini et al., 2005). The TS primarily processes auditory and lateral line information but also contains visual- and somatosensory-sensitive neurons in some fishes (Schellart, 1983; Schellart & Kroese, 1989; Yamamoto et al., 2010). Thus, NO signaling in regions of the midbrain may be involved in integrating information from multiple sensory systems to relay it to forebrain decision centers and to coordinate with motor circuits needed for behavioral displays.

The expression of *nnos* in the rhombencephalon varies in presence and quantity across fishes (Giraldez-Perez et al., 2009). We found stained cells in the granular and molecular layers of the cerebellum of *A. burtoni*, a pattern similar to that of carp (Biswas et al., 2015). As in *A. burtoni*, several species of teleosts express *nnos* in the Purkinje cell layer of the cerebellum, including zebrafish (Holmqvist et al., 2000; Masini et al., 2005). Gars express *nnos* in the cerebellum, as well as the central gray (López et al., 2017). In a quantification of NNOS activity (measured as protein levels), radioactivity for NNOS was detected in the medulla oblongata of both trout and goldfish but only in the cerebellar regions of goldfish (Virgili et al., 2001). Scattered cells throughout the sensory region of the vagal lobes in *A. burtoni*, as well as in SGn and SVn, suggest roles in visceral sensory processing and gustation. This distribution pattern may be conserved, as nNOS is also expressed in vagal regions of mammals (Krowicki et al., 1997; Lin et al., 1998). Our RT-PCR also revealed strong expression in the cerebellum, hindbrain, and spinal cord, suggesting that NO signaling is also involved in diverse functions controlled by the rhombencephalon.

As in teleosts, the distribution of *nnos* is widespread across the brains of tetrapods, but there is extensive variation in its distribution across different brain regions among taxa (Brüning & Mayer, 1996; Brüning et al., 1994; Chong et al., 2019; González et al., 2002; Gotti et al., 2005; Huynh & Boyd, 2007). The variation of *nnos* among and within vertebrate classes may be due to selection on NO-signaling pathways of a particular niche (Virgili et al., 2001). Further comparative studies of closely related species that consider adaptations to environments may help deduce how NO signaling pathways evolved within brain regions. Cichlids may be an amenable system for this pursuit due to their radiation into a wide variety of habitats and their diverse reproductive and parental care strategies that exert selective pressures on different aspects of the brain.

## 4.2 | *nnos* expression and roles in sensory tissues

In addition to its roles in the brain, NO is present in the sensory organs of many animals. We found *nnos* within the inner nuclear layer of the retina of *A. burtoni*, presumably in a type of amacrine cell. nNOS immunoreactivity is also found in amacrine cells of the inner nuclear layer in other species, suggesting a role for NO signaling in retinal physiology and vision (Cao & Eldred, 2001; Perez et al., 1995). Across vertebrates, nNOS-expressing cells are detected in amacrine, horizontal, ganglion, bipolar, Müller, photoreceptor, and other cells of the retina in different species (Vielma et al., 2012). These

studies demonstrate important roles for NO signaling in the retina of all vertebrates, but localization in different cell types across species may suggest diverse functions that could in part depend on habitat and relative reliance on vision for feeding, navigation, predator avoidance, and social interactions. NO enables multiple actions within the retina, including modulating light/dark adaptation, modulation of other neurotransmitters and ion conductance (Vielma et al., 2012), and regulation of vascularization (Li et al., 2017). As such, the visual capacities of animals, which shift among social and reproductive contexts, may be modulated by the activity of nNOS in the retina.

We were unable to successfully detect *nnos* in the olfactory epithelial tissues through multiple methods focused on measuring mRNA, in contrast to studies in several other vertebrates using primarily immunohistochemistry techniques. However, as mentioned above, the use of NADPH-d and some nNOS antibodies in olfactory tissues may not be a reliable indicator of nNOS presence. Considering that *nnos*-deficient mutants are impaired in olfactory-based tasks (Pavesi et al., 2013), the lack of *nnos* mRNA in the olfactory epithelium of *A. burtoni* may merely indicate that NO serves as a neurotransmitter in more central areas of the olfactory system because we do find *nnos* expression in the OBs and primary olfactory processing regions of the forebrain (e.g., Dp, Vv).

We also tested for *nnos* expression in the saccule of the inner ear because *A. burtoni* males produce courtship sounds that provide important information to females during reproduction, and the detection of these sounds may also be used by subordinate males to monitor courtship activities of territory-holding dominant males (Maruska et al., 2012). However, we did not detect *nnos* in the *A. burtoni* saccules, suggesting that NO is not used as a transmitter in the peripheral auditory system, but *nnos*-expressing cells in central auditory processing regions such as octavolateralis nuclei, torus semicircularis, and thalamic regions suggest it may play a role at higher processing levels. There is evidence for nNOS expression and NO production in the inner ear of many tetrapods, including axolotls (Flores et al., 1996), frogs (Heinrich, 2003), and mammals (rats: Yamane et al., 1997; guinea pigs: Wang et al., 2005), and excessive NO production is thought to play a role in inner ear disorders (Takumida & Anniko, 2002). While NO signaling may not be a common mechanism involved in peripheral auditory processing, more comparative studies are needed.

## 4.3 | Reproductive state and social status differences in *nnos* mRNA expression

We did not find any obvious differences in the overall localization patterns of *nnos*-expressing cells in the brain between sexes or among reproductive statuses within each sex, unlike several other signaling molecules in the brain that differ among these groups in *A. burtoni* (Maruska, Butler, Anselmo, et al., 2020; Maruska, Butler, Field, et al., 2020). However, this is not surprising given the widespread distribution and general transmitter functions of nitrergic signaling in the vertebrate brain. Future studies that quantify mRNA expression levels in distinct nuclei across sex and reproductive conditions are needed to

examine localized changes in *nnos* expression that may modulate NO production and release in specific regions.

*nnos* mRNA levels in the eye change with social status and reproductive state in *A. burtoni* males but in not females. Unlike the differences in *nnos* observed here, several other modulators of the visual system are similarly expressed in the eye between dominant and subordinate males (Butler et al., 2019). Different levels of *nnos* expression in the retina suggest that this neuromodulator plays roles unrelated to chromatic sensitivities, as spectral sensitivity is similar among males. The effects of NO may instead regulate horizontal-cell activity and thus receptive-field size in the retina (Cudeiro & Rivadulla, 1999) or modulate other visual capabilities, such as contrast discrimination or acuity. Discerning spatial dimensions may be more important than color for males that compete for status, as opponent size is a factor in dominant male aggression (Alward et al., 2021). Furthermore, dominant courting males may not rely on color detection for mating but rather on other visual attributes, such as female affiliation behaviors, movements, and body shape, to discern gravidity. Experimental work evaluating how *nnos* expression changes in response to different social stimuli will also be of great value.

*nnos* expression in the OBs was higher in dominant males than in subordinate males. In dominant males, olfactory stimulation invokes courtship toward females and aggression toward rival males (Field et al., 2018; Maruska & Fernald, 2012). However, for subordinates, olfaction may serve primarily to detect the social status of potential competitors because their olfactory forebrain neurons are more responsive to olfactory signals from males rather than those from females (Nikonov & Maruska, 2019). While this and other studies demonstrate *nnos*-expressing cells in the eye and olfactory system, further experimental work is needed to understand the mechanisms by which nNOS activity contributes to sensory perceptions from a functional perspective.

## 5 | CONCLUSIONS

Here, we describe the distribution of *nnos*-expressing cells throughout the brain, eyes, and olfactory system of a mouthbrooding cichlid and find patterns that appear to be conserved with other aquatic vertebrates. We also demonstrate quantitative differences in the expression of the *nnos* gene between the sexes (in eyes), as well as between dominant and subordinate social status of males (in OBs and eyes), but not among the reproductive states of females (in eyes). These findings suggest that NO is a potential effector of the nervous system in relation to sensory processing, social interactions, and reproductive physiology. Further studies investigating how the activity of *nnos* differs among social and reproductive behavioral contexts would inform our understanding of its role in mediating plasticity across sensory and reproductive systems.

## AUTHOR CONTRIBUTIONS

All authors had full access to the data, take responsibility for the integrity of the data analysis, and approved the final manuscript. Karen P. Maruska, Emily J. Ray, and Robert B. Mobley were involved in study concept and design. Robert B. Mobley, Emily J. Ray, and Karen P. Maruska performed ISH and qPCR experiments and analysis. Robert B. Mobley, Emily J. Ray, and Karen P. Maruska analyzed and interpreted the data. Robert B. Mobley, Emily J. Ray, and Karen P. Maruska were involved in manuscript drafts and editing to final form. Karen P. Maruska provided equipment, resources, and funding.

## CONFLICT OF INTEREST

The authors declare no conflict of interest.

## DATA AVAILABILITY STATEMENT

The data that support the findings of this study are available from the corresponding author upon reasonable request.

## ORCID

*Robert B. Mobley* https://orcid.org/0000-0001-9114-1076
*Emily J. Ray* https://orcid.org/0000-0003-3968-1109
*Karen P. Maruska* https://orcid.org/0000-0003-2425-872X

## REFERENCES

Alderton, W. K., Cooper, C. E., & Knowles, R. G. (2001). Nitric oxide synthases: Structure, function and inhibition. *Biochemical Journal*, *357*, 593–615.

Alward, B. A., Cathers, P. H., Blakkan, D. M., Hoadley, A. P., & Fernald, R. D. (2021). A behavioral logic underlying aggression in an African cichlid fish. *Ethology*, *127*(7), 572–581. https://doi.org/10.1111/eth.13164

Ambe, K., Watanabe, H., Takahashi, S., Nakagawa, T., & Sasaki, J. (2016). Production and physiological role of NO in the oral cavity. *Japanese Dental Science Review*, *52*(1), 14–21. https://doi.org/10.1016/j.jdsr.2015.08.001

Ando, H., Shi, Q., Kusakabe, T., Ohya, T., Suzuki, N., & Urano, A. (2004). Localization of mRNAs encoding $\alpha$ and $\beta$ subunits of soluble guanylyl cyclase in the brain of rainbow trout: Comparison with the distribution of neuronal nitric oxide synthase. *Brain Research*, *1013*(1), 13–29. https://doi.org/10.1016/j.brainres.2004.03.063

Bedenbaugh, M. N. (2018). *The role of KNDy neurons and neuronal nitric oxide synthase in the control of reproduction in female sheep and nonhuman primates* [PhD Dissertation, West Virginia University Libraries]. https://doi.org/10.33915/etd.5174

Biswas, S. P., Jadhao, A. G., Bhoyar, R. C., Palande, N. V., & Sinh, D. P. (2015). Neuroanatomical localization of nitric oxide synthase (nNOS) in the central nervous system of carp, *Labeo rohita* during post-embryonic development. *International Journal of Developmental Neuroscience*, *46*(1), 14–26. https://doi.org/10.1016/j.ijdevneu.2015.06.004

Bordieri, L., Bonaccorsi di Patti, M. C., Miele, R., & Cioni, C. (2005). Partial cloning of neuronal nitric oxide synthase (nNOS) cDNA and regional distribution of nNOS mRNA in the central nervous system of the Nile

tilapia *Oreochromis niloticus*. *Molecular Brain Research*, *142*(2), 123–133. https://doi.org/10.1016/j.molbrainres.2005.09.018

Brüning, G., & Mayer, B. (1996). Localization of nitric oxide synthase in the brain of the frog, *Xenopus laevis*. *Brain Research*, *741*(1–2), 331–343. https://doi.org/10.1016/S0006-8993(96)00944-4

Brüning, G., Wiese, S., & Mayer, B. (1994). Nitric oxide synthase in the brain of the turtle *Pseudemys scripta elegans*: Nitric oxide synthase in turtle brain. *Journal of Comparative Neurology*, *348*(2), 183–206. https://doi.org/10.1002/cne.903480203

Burmeister, S. S., Munshi, R. G., & Fernald, R. D. (2009). Cytoarchitecture of a cichlid fish telencephalon. *Brain, Behavior and Evolution*, *74*(2), 110–120. https://doi.org/10.1159/000235613

Butler, J. M., & Maruska, K. P. (2016). The mechanosensory lateral line system mediates activation of socially-relevant brain regions during territorial interactions. *Frontiers in Behavioral Neuroscience*, *10*, 93. https://doi.org/10.3389/fnbeh.2016.00093

Butler, J. M., & Maruska, K. P. (2019). Expression of *tachykinin3* and related reproductive markers in the brain of the African cichlid fish *Astatotilapia burtoni*. *Journal of Comparative Neurology*, *527*(7), 1210–1227. https://doi.org/10.1002/cne.24622

Butler, J. M., Whitlow, S. M., Rogers, L. S., Putland, R. L., Mensinger, A. F., & Maruska, K. P. (2019). Reproductive state-dependent plasticity in the visual system of an African cichlid fish. *Hormones and Behavior*, *114*, 104539. https://doi.org/10.1016/j.yhbeh.2019.06.003

Cao, L., & Eldred, W. D. (2001). Subcellular localization of neuronal nitric oxide synthase in turtle retina: Electron immunocytochemistry. *Visual Neuroscience*, *18*(6), 949–960. https://doi.org/10.1017/S0952523801186128

Chang, J. P., & Pemberton, J. G. (2018). Comparative aspects of GnRH-Stimulated signal transduction in the vertebrate pituitary—Contributions from teleost model systems. *Molecular and Cellular Endocrinology*, *463*, 142–167. https://doi.org/10.1016/j.mce.2017.06.002

Chong, P. S., Poon, C. H., Fung, M. L., Guan, L., Steinbusch, H. W. M., Chan, Y.-S., Lim, W. L., & Lim, L. W. (2019). Distribution of neuronal nitric oxide synthase immunoreactivity in adult male Sprague-Dawley rat brain. *Acta Histochemica*, *121*(8), 151437. https://doi.org/10.1016/j.acthis.2019.08.004

Cudeiro, J., & Rivadulla, C. (1999). Sight and insight—On the physiological role of nitric oxide in the visual system. *Trends in Neurosciences*, *22*(3), 109–116. https://doi.org/10.1016/S0166-2236(98)01299-5

Dixit, V. D., & Parvizi, N. (2001). Nitric oxide and the control of reproduction. *Animal Reproduction Science*, *65*(1–2), 1–16. https://doi.org/10.1016/S0378-4320(00)00224-4

Escobar, S., Servili, A., Espigares, F., Gueguen, M.-M., Brocal, I., Felip, A., Gómez, A., Carrillo, M., Zanuy, S., & Kah, O. (2013). Expression of kisspeptins and kiss receptors suggests a large range of functions for kisspeptin systems in the brain of the European sea bass. *PLoS One*, *8*(7), e70177. https://doi.org/10.1371/journal.pone.0070177

Ferrando, S., Gallus, L., Gambardella, C., Amaroli, A., Cutolo, A., Masini, M. A., Vallarino, M., & Vacchi, M. (2012). Neuronal nitric oxide synthase (nNOS) immunoreactivity in the olfactory system of a cartilaginous fish. *Journal of Chemical Neuroanatomy*, *43*(2), 133–140. https://doi.org/10.1016/j.jchemneu.2012.03.005

Fessenden, J. D., Altschuler, R. A., Seasholtz, A. F., & Schacht, J. (1999). Nitric oxide/cyclic guanosine monophosphate pathway in the peripheral and central auditory system of the rat. *Journal of Comparative Neurology*, *404*(1), 52–63.

Field, K. E., McVicker, C. T., & Maruska, K. P. (2018). Sexually-relevant visual and chemosensory signals induce distinct behaviors and neural activation patterns in the social African cichlid, *Astatotilapia burtoni*. *Frontiers in Behavioral Neuroscience*, *12*, 267. https://doi.org/10.3389/fnbeh.2018.00267

Flores, A., León-Olea, M., Vega, R., & Soto, E. (1996). Histochemistry and role of nitric oxide synthase in the amphibian (*Ambystoma tigrinum*) inner ear. *Neuroscience Letters*, 205(2), 131–134. https://doi.org/10.1016/0304-3940(96)12398-3

Gaikwad, A., Biju, K. C., Barsagade, V., Bhute, Y., & Subhedar, N. (2009). Neuronal nitric oxide synthase in the olfactory system, forebrain, pituitary and retina of the adult teleost *Clarias batrachus*. *Journal of Chemical Neuroanatomy*, 37(3), 170–181. https://doi.org/10.1016/j.jchemneu.2008.12.006

Giraldez-Perez, R. M., Gaytan, S. P., Torres, B., & Pasaro, R. (2009). Co-localization of nitric oxide synthase and choline acetyltransferase in the brain of the goldfish (*Carassius auratus*). *Journal of Chemical Neuroanatomy*, 37(1), 1–17. https://doi.org/10.1016/j.jchemneu.2008.08.004

González, A., Moreno, N., & López, J. M. (2002). Distribution of NADPH-diaphorase/nitric oxide synthase in the brain of the caecilian *Dermophis mexicanus* (Amphibia: Gymnophiona): Comparative aspects in amphibians. *Brain, Behavior and Evolution*, 60(2), 80–100. https://doi.org/10.1159/000065204

Gotti, S., Sica, M., Viglietti-Panzica, C., & Panzica, G. (2005). Distribution of nitric oxide synthase immunoreactivity in the mouse brain. *Microscopy Research and Technique*, 68(1), 13–35. https://doi.org/10.1002/jemt.20219

Grone, B. P., Butler, J. M., Wayne, C. R., & Maruska, K. P. (2021). Expression patterns and evolution of urocortin and corticotropin-releasing hormone genes in a cichlid fish. *Journal of Comparative Neurology*, 529(10), 2596–2619. https://doi.org/10.1002/cne.25113

Grone, B. P., & Maruska, K. P. (2015). Divergent evolution of two corticotropin-releasing hormone (CRH) genes in teleost fishes. *Frontiers in Neuroscience*, 9, 365. https://doi.org/10.3389/fnins.2015.00365

Grone, B. P., Maruska, K. P., Korzan, W. J., & Fernald, R. D. (2010). Social status regulates kisspeptin receptor mRNA in the brain of *Astatotilapia burtoni*. *General and Comparative Endocrinology*, 169(1), 98–107. https://doi.org/10.1016/j.ygcen.2010.07.018

Günther, A. (1894). Second report on the reptiles, batrachians, and fishes transmitted by Mr. H. H. Johnston, C. B., from British Central Africa. *Proceedings of the General Meetings for Scientific Business of the Zoological Society of London*, 4, 616–628.

Heinrich, U.-R. (2003). Localization of the two constitutively expressed nitric oxide synthase isoforms (nNOS and eNOS) in the same cell types in the saccule maculae of the frog *Rana pipiens* by immunoelectron microscopy: Evidence for a back-up system? *Journal of Electron Microscopy*, 52(2), 197–206. https://doi.org/10.1093/jmicro/52.2.197

Holmqvist, B. (2004). The early ontogeny of neuronal nitric oxide synthase systems in the zebrafish. *Journal of Experimental Biology*, 207(6), 923–935. https://doi.org/10.1242/jeb.00845

Holmqvist, B., Ellingsen, B., Alm, P., & Forsell, J. (2000). Identification and distribution of nitric oxide synthase in the brain of adult zebrafish. *Neuroscience Letters*, 292, 119–122.

Huynh, P., & Boyd, S. K. (2007). Nitric oxide synthase and NADPH diaphorase distribution in the bullfrog (*Rana catesbeiana*) CNS: Pathways and functional implications. *Brain, Behavior and Evolution*, 70(3), 145–163. https://doi.org/10.1159/000104306

Jadhao, A. G., & Malz, C. R. (2003). Localization of the neuronal form of nitric oxide synthase (bNOS) in the diencephalon and pituitary gland of the catfish, *Synodontis multipunctatus*: An immunocytochemical study. *General and Comparative Endocrinology*, 132(2), 278–283. https://doi.org/10.1016/S0016-6480(03)00096-0

Jadhao, A. G., & Malz, C. R. (2004). Nicotinamide adenine dinucleotide phosphate (NADPH)-diaphorase activity in the brain of a cichlid fish, with remarkable findings in the entopeduncular nucleus: A histochemical study. *Journal of Chemical Neuroanatomy*, 27(2), 75–86. https://doi.org/10.1016/j.jchemneu.2003.12.001

Jüch, M., Smalla, K.-H., Kähne, T., Lubec, G., Tischmeyer, W., Gundelfinger, E. D., & Engelmann, M. (2009). Congenital lack of nNOS impairs long-term social recognition memory and alters the olfactory bulb proteome. *Neurobiology of Learning and Memory*, 92(4), 469–484. https://doi.org/10.1016/j.nlm.2009.06.004

Kelley, J. B., Balda, M. A., Anderson, K. L., & Itzhak, Y. (2009). Impairments in fear conditioning in mice lacking the nNOS gene. *Learning & Memory*, 16(6), 371–378. https://doi.org/10.1101/lm.1329209

Kirchner, L., Weitzdoerfer, R., Hoeger, H., Url, A., Schmidt, P., Engelmann, M., Villar, S. R., Fountoulakis, M., Lubec, G., & Lubec, B. (2004). Impaired cognitive performance in neuronal nitric oxide synthase knockout mice is associated with hippocampal protein derangements. *Nitric Oxide*, 11(4), 316–330. https://doi.org/10.1016/j.niox.2004.10.005

Kishimoto, J., Keverne, E. B., Hardwick, J., & Emson, P. C. (1993). Localization of nitric oxide synthase in the mouse olfactory and vomeronasal system: A histochemical, immunological and in situ hybridization study. *European Journal of Neuroscience*, 5(12), 1684–1694. https://doi.org/10.1111/j.1460-9568.1993.tb00236.x

Krowicki, Z. K., Sharkey, K. A., Serron, S. C., Nathan, N. A., & Hornby, P. J. (1997). Distribution of nitric oxide synthase in rat dorsal vagal complex and effects of microinjection of nitric oxide compounds upon gastric motor function. *The Journal of Comparative Neurology*, 377(1), 49–69. https://doi.org/10.1002/(SICI)1096-9861(19970106)377:149::AID-CNE63.0.CO;2-J

Lema, S. C., & Nevitt, G. A. (2001). Re-evaluating NADPH-diaphorase histochemistry as an indicator of nitric oxide synthase: An examination of the olfactory system of coho salmon (*Oncorhynchus kisutch*). *Neuroscience Letters*, 313(1–2), 1–4.

Li, C., Taylor, C., Guley, N., Del Mar, N., Fitzgerald, M. E., & Reiner, A. (2017). Effect of neuronal nitric oxide synthase deletion on choroidal blood flow and retinal morphology and function. *Investigative Ophthalmology & Visual Science*, 58(8), 3039–3039.

Lin, L.-H., Cassell, M. D., Sandra, A., & Talman, W. T. (1998). Direct evidence for nitric oxide synthase in vagal afferents to the nucleus tractus solitarii. *Neuroscience*, 84(2), 549–558. https://doi.org/10.1016/S0306-4522(97)00501-0

López, J. M., Lozano, D., Morales, L., & González, A. (2017). Pattern of nitrergic neuronal system organization in the brain of two holostean fishes (Actinopterygii: Ginglymodi). *Brain, Behavior and Evolution*, 89(2), 117–152. https://doi.org/10.1159/000455964

López, J. M., Lozano, D., Morona, R., & González, A. (2016). Organization of the nitrergic neuronal system in the primitive bony fishes *Polypterus senegalus* and *Erpetoichthys calabaricus* (Actinopterygii: Cladistia): Nitric Oxide in the Brain of Cladistians. *Journal of Comparative Neurology*, 524(9), 1770–1804. https://doi.org/10.1002/cne.23922

López, J. M., Morona, R., & González, A. (2019). Pattern of nitrergic cells and fibers organization in the central nervous system of the Australian lungfish, *Neoceratodus forsteri* (Sarcopterygii: Dipnoi). *Journal of Comparative Neurology*, 527(11), 1771–1800. https://doi.org/10.1002/cne.24645

Luo, D., Ganesh, S., & Koolaard, J. (2018). Predictmeans: Calculate predicted means for linear models. https://CRAN.R-project.org/package=predictmeans

Maruska, K. P., & Butler, J. M. (2021). Reproductive- and social-state plasticity of multiple sensory systems in a cichlid fish. *Integrative and Comparative Biology*, 61, 249–268. https://doi.org/10.1093/icb/icab062

Maruska, K. P., Butler, J. M., Anselmo, C., & Tandukar, G. (2020). Distribution of aromatase in the brain of the African cichlid fish *Astatotilapia burtoni*: Aromatase expression, but not estrogen receptors, varies with female reproductive-state. *Journal of Comparative Neurology*, 528(15), 2499–2522.

Maruska, K. P., Butler, J. M., Field, K. E., Forester, C., & Augustus, A. (2020). Neural activation patterns associated with maternal mouthbrooding and energetic state in an African cichlid fish. *Neuroscience*, 446, 199–212. https://doi.org/10.1016/j.neuroscience.2020.07.025

Maruska, K. P., Butler, J. M., Field, K. E., & Porter, D. T. (2017). Localization of glutamatergic, GABAergic, and cholinergic neurons in the brain of the African cichlid fish, *Astatotilapia burtoni*: Neurotransmitter localization in

cichlid brain. *Journal of Comparative Neurology*, *525*(3), 610–638. https://doi.org/10.1002/cne.24092

Maruska, K. P., & Fernald, R. D. (2010a). Steroid receptor expression in the fish inner ear varies with sex, social status, and reproductive state. *BMC Neuroscience*, *11*(1), 1–17.

Maruska, K. P., & Fernald, R. D. (2010b). Reproductive status regulates expression of sex steroid and GnRH receptors in the olfactory bulb. *Behavioural Brain Research*, *213*(2), 208–217. https://doi.org/10.1016/j.bbr.2010.04.058

Maruska, K. P., & Fernald, R. D. (2012). Contextual chemosensory urine signaling in an African cichlid fish. *Journal of Experimental Biology*, *215*(1), 68–74. https://doi.org/10.1242/jeb.062794

Maruska, K. P., & Fernald, R. D. (2018). *Astatotilapia burtoni*: A model system for analyzing the neurobiology of behavior. *ACS Chemical Neuroscience*, *9*(8), 1951–1962. https://doi.org/10.1021/acschemneuro.7b00496

Maruska, K. P., Ung, U. S., & Fernald, R. D. (2012). The African cichlid fish *Astatotilapia burtoni* uses acoustic communication for reproduction: Sound production, hearing, and behavioral significance. *PLoS One*, *7*(5), e37612. https://doi.org/10.1371/journal.pone.0037612

Masini, M. A., Sturla, M., Ricci, F., & Uva, B. M. (2005). Identification and distribution of nitric oxide synthase in the brain of adult Antarctic teleosts. *Polar Biology*, *29*(1), 23–26. https://doi.org/10.1007/s00300-005-0033-1

Muñoz-Cueto, J. A. (2001). *An atlas of the brain of the gilthead seabream (*Sparus aurata*)*. Maryland Sea Grant.

Navarrete-Palacios, E., Hudson, R., Reyes-Guerrero, G., & Guevara-Guzmán, R. (2003). Lower olfactory threshold during the ovulatory phase of the menstrual cycle. *Biological Psychology*, *63*(3), 269–279. https://doi.org/10.1016/S0301-0511(03)00076-0

Nelson, R. J., Demas, G. E., Huang, P. L., Fishman, M. C., Dawson, V. L., Dawson, T. M., & Snyder, S. H. (1995). Behavioural abnormalities in male mice lacking neuronal nitric oxide synthase. *Nature*, *378*(6555), 383–386. https://doi.org/10.1038/378383a0

Nikonov, A. A., & Maruska, K. P. (2019). Male dominance status regulates odor-evoked processing in the forebrain of a cichlid fish. *Scientific Reports*, *9*(1), 1–17. https://doi.org/10.1038/s41598-019-41521-6

Ohga, H., Selvaraj, S., & Matsuyama, M. (2018). The roles of kisspeptin system in the reproductive physiology of fish with special reference to chub mackerel studies as main axis. *Frontiers in Endocrinology*, *9*, 147. https://doi.org/10.3389/fendo.2018.00147

Ota, D., Downing, J. E. G., & Cook, J. E. (1999). Neuronal and glial cell types revealed by NADPH-diaphorase histochemistry in the retina of a teleost fish, the grass goby (*Zosterisessor ophiocephalus*, Perciformes, Gobiidae). *Anatomy and Embryology*, *200*(5), 487–494. https://doi.org/10.1007/s004290050297

Pavesi, E., Heldt, S. A., & Fletcher, M. L. (2013). Neuronal nitric-oxide synthase deficiency impairs the long-term memory of olfactory fear learning and increases odor generalization. *Learning & Memory*, *20*(9), 482–490. https://doi.org/10.1101/lm.031450.113

Perez, M. T. R., Larsson, B., Alm, P., Andersson, K.-E., & Ehinger, B. (1995). Localisation of neuronal nitric oxide synthase-immunoreactivity in rat and rabbit retinas. *Experimental Brain Research*, *104*(2), 207–217. https://doi.org/10.1007/BF00242007

Porter, D. T., Roberts, D. A., & Maruska, K. P. (2017). Distribution and female reproductive state differences in orexigenic and anorexigenic neurons in the brain of the mouth brooding African cichlid fish, *Astatotilapia burtoni*. *Journal of Comparative Neurology*, *525*(14), 3126–3157. https://doi.org/10.1002/cne.24268

R Core Team. (2021). *R: A Language and Environment for Statistical Computing*. R Foundation for Statistical Computing. https://www.R-project.org/

Sánchez-Islas, E., & León-Olea, M. (2001). Histochemical and immunohistochemical localization of neuronal nitric oxide synthase in the olfactory epithelium of the axolotl, *Ambystoma mexicanum*. *Nitric Oxide*, *5*(4), 302–316. https://doi.org/10.1006/niox.2001.0347

Schellart, N. A. M. (1983). Acousticolateral and visual processing and their interaction in the torus semicircularis of the trout, *Salmo gairdneri*. *Neuroscience Letters*, *42*(1), 39–44. https://doi.org/10.1016/0304-3940(83)90418-4

Schellart, N. A. M., & Kroese, A. B. A. (1989). Interrelationship of acousticolateral and visual systems in the teleost midbrain. In Coombs, S., Görner, P., & Münz, H. (Eds.), *The mechanosensory lateral line* (pp. 421–443). Springer New York. https://doi.org/10.1007/978-1-4612-3560-6_21

Sica, M., Martini, M., Viglietti-Panzica, C., & Panzica, G. (2009). Estrous cycle influences the expression of neuronal nitric oxide synthase in the hypothalamus and limbic system of female mice. *BMC Neuroscience*, *10*(1), 78. https://doi.org/10.1186/1471-2202-10-78

Sisneros, J. A., & Bass, A. H. (2003). Seasonal plasticity of peripheral auditory frequency sensitivity. *The Journal of Neuroscience*, *23*(3), 1049–1058. https://doi.org/10.1523/JNEUROSCI.23-03-01049.2003

Sülz, L., Astorga, G., Bellette, B., Iturriaga, R., Mackay-Sim, A., & Bacigalupo, J. (2009). Nitric oxide regulates neurogenesis in adult olfactory epithelium in vitro. *Nitric Oxide*, *20*(4), 238–252. https://doi.org/10.1016/j.niox.2009.01.004

Takumida, M., & Anniko, M. (2002). Nitric oxide in the inner ear. *Current Opinion in Neurology*, *15*(1), 11–15. https://doi.org/10.1097/00019052-200202000-00003

Trainor, B. C., Workman, J. L., Jessen, R., & Nelson, R. J. (2007). Impaired nitric oxide synthase signaling dissociates social investigation and aggression. *Behavioral Neuroscience*, *121*(2), 362–369. https://doi.org/10.1037/0735-7044.121.2.362

Vielma, A. H., Retamal, M. A., & Schmachtenberg, O. (2012). Nitric oxide signaling in the retina: What have we learned in two decades? *Brain Research*, *1430*, 112–125. https://doi.org/10.1016/j.brainres.2011.10.045

Virgili, M., Poli, A., Beraudi, A., Giuliani, A., & Villani, L. (2001). Regional distribution of nitric oxide synthase and NADPH-diaphorase activities in the central nervous system of teleosts. *Brain Research*, *901*(1–2), 202–207. https://doi.org/10.1016/S0006-8993(01)02357-5

Wang, A., Tang, H., Zhang, Z., Lianming, L., & Hua, M. (2005). Localization and expression of three nitric oxide synthase isoforms in the cochlea of guinea pigs and the effects in the hearing process of inner ear. *Chinese Journal of Tissue Engineering Research*, *9*(37), 160–161.

Whitaker, K. W., Neumeister, H., Huffman, L. S., Kidd, C. E., Preuss, T., & Hofmann, H. A. (2011). Serotonergic modulation of startle-escape plasticity in an African cichlid fish: A single-cell molecular and physiological analysis of a vital neural circuit. *Journal of Neurophysiology*, *106*(1), 127–137. https://doi.org/10.1152/jn.01126.2010

Wullimann, M. F., Rupp, B., & Reichert, H. (1996). *Neuroanatomy of the Zebrafish Brain*. Birkhäuser Basel. https://doi.org/10.1007/978-3-0348-8979-7

Yamamoto, N., Kato, T., Okada, Y., & Somiya, H. (2010). Somatosensory nucleus in the torus semicircularis of cyprinid teleosts. *The Journal of Comparative Neurology*, *518*, 2475–2502. https://doi.org/10.1002/cne.22348

Yonehara, N., Kudo, C., & Kamisaki, Y. (2003). Involvement of NMDA–nitric oxide pathways in the development of tactile hypersensitivity evoked by the loose-ligation of inferior alveolar nerves in rats. *Brain Research*, *963*(1–2), 232–243. https://doi.org/10.1016/S0006-8993(02)03983-5

Yamane, H., Takayama, M., Konishi, K., Iguchi, H., Shibata, S., Sunami, K., & Nakai, Y. (1997). Nitric oxide synthase and contractile protein in the rat cochlear lateral wall: possible role of nitric oxide in regulation of strial blood flow. *Hearing research*, *108*(1–2), 65–73.

Zaccone, G. (2002). Immunohistochemical investigation of the nitrergic system in the taste organ of the frog, *Rana esculenta*. *Chemical Senses*, *27*(9), 825–830. https://doi.org/10.1093/chemse/27.9.825

Zhao, S., & Fernald, R. D. (2005). Comprehensive algorithm for quantitative real-time polymerase chain reaction. *Journal of Computational Biology*, *12*(8), 1047–1064. https://doi.org/10.1089/cmb.2005.12.1047

Zoubovsky, S. P., Pogorelov, V. M., Taniguchi, Y., Kim, S.-H., Yoon, P., Nwulia, E., Sawa, A., Pletnikov, M. V., & Kamiya, A. (2011). Working memory deficits in neuronal nitric oxide synthase knockout mice: Potential impairments in prefrontal cortex mediated cognitive function. *Biochemical and Biophysical Research Communications*, *408*(4), 707–712. https://doi.org/10.1016/j.bbrc.2011.04.097